These results suggest that the liposome-disrupting activity of the protein encoded by NT01CX2047 (henceforth termed liposomase) is due to interaction of its lipid-binding domain with the liposomal membrane and the consequent alteration of bilayer structure. This explains why a lipase, which has little phospholipase activity, can disrupt liposomes, which contain phospholipids but no triacylglycerides.

In principle, the approach described here should be applicable to any chemotherapeutic drug that can be encapsulated in a liposome. Indeed, when we repeated the preclinical efficacy experiments with liposomes carrying CPT-11 (irinotecan), a topoisomerase inhibitor widely used in cancer therapy, we obtained results similar to those in the Doxil experiments (fig. S9). Both CT26 mouse tumors and HCT116 human xenografts were relatively resistant to CPT-11 when the drug was administered alone in unencapsulated or liposome-encapsulated form. However, when liposomal CPT-11 was delivered in combination with *C. novyi-NT* spores, all tumors regressed and more than 60% of the mice survived for at least 3 months (fig. S9). Notably, the combination therapy was effective against small (136 mm^3 in volume) as well as large tumors. In previous studies, small tumors were resistant to bacteriolytic therapies because they had relatively small regions of necrosis (*15*). Importantly, mice treated with *C. novyi-NT* and either Doxil or CPT-11 tolerated the treatments well and did not generally suffer toxicities or weight loss (fig. S10).

We have not excluded the possibility that other secreted factors may contribute to the liposome-disrupting activity. However, the data reported here suggest that liposomase substantially contributes to the therapeutic effects observed in vivo. The identification and cloning of liposomase opens the door to therapeutic strategies in addition to those based on bacteriolysis. For example, liposomase could be attached to antibodies or encoded within vectors used for gene therapy (*3*, *4*). Because virtually any therapeutic agent can be packaged in liposomes and can thereby act as a "prodrug," liposomase offers a number of possibilities for the specific delivery of drugs to tumors.

References and Notes

1. D. D. Von Hoff, A.-R. Hanauske, in *Cancer Medicine*, D. W. Kufe *et al.*, Eds. (BC Decker, London, 2006), pp. 600–616.
2. C. Sawyers, *Nature* **432**, 294 (2004).
3. S. V. Govindan, G. L. Griffiths, H. J. Hansen, I. D. Horak, D. M. Goldenberg, *Technol. Cancer Res. Treat.* **4**, 375 (2005).
4. M. Yamamoto, D. T. Curiel, *Technol. Cancer Res. Treat.* **4**, 315 (2005).
5. R. Kerbel, J. Folkman, *Nat. Rev. Cancer* **2**, 727 (2002).
6. R. K. Jain, D. G. Duda, J. W. Clark, J. S. Loeffler, *Nat. Clin. Pract. Oncol.* **3**, 24 (2006).
7. G. Thurston *et al.*, *J. Clin. Invest.* **101**, 1401 (1998).
8. H. Hashizume *et al.*, *Am. J. Pathol.* **156**, 1363 (2000).
9. D. C. Drummond, O. Meyer, K. Hong, D. B. Kirpotin, D. Papahadjopoulos, *Pharmacol. Rev.* **51**, 691 (1999).
10. J. Fang, T. Sawa, H. Maeda, *Adv. Exp. Med. Biol.* **519**, 29 (2003).
11. R. M. Ryan, J. Green, C. E. Lewis, *Bioessays* **28**, 84 (2006).
12. S. Barbe, L. Van Mellaert, J. Anne, *J. Appl. Microbiol.* **101**, 571 (2006).
13. J. Sakurai, M. Nagahama, M. Oda, *J. Biochem. (Tokyo)* **136**, 569 (2004).
14. D. Papahadjopoulos *et al.*, *Proc. Natl. Acad. Sci. U.S.A.* **88**, 11460 (1991).
15. L. H. Dang, C. Bettegowda, D. L. Huso, K. W. Kinzler, B. Vogelstein, *Proc. Natl. Acad. Sci. U.S.A.* **98**, 15155 (2001); published online 27 November 2001.
16. N. Agrawal *et al.*, *Proc. Natl. Acad. Sci. U.S.A.* **101**, 15172 (2004).
17. C. Bettegowda *et al.*, *Nat. Biotechnol.*, in press.
18. Materials and methods are available as supporting material on *Science* Online.
19. K. E. Jaeger, B. W. Dijkstra, M. T. Reetz, *Annu. Rev. Microbiol.* **53**, 315 (1999).

20. We thank L. Watson for assistance with animal experiments, S. Szabo for sequencing, D. Mamelak for assistance with proteomic analysis, K. Leong for advice on particle sizing, and P. Singh and S. Chandran for advice on fluorescence polarization. This work was supported by the Virginia and D. K. Ludwig Fund for Cancer Research, the Commonwealth Foundation, the Miracle Foundation, and NIH grant CA062924.

Supporting Online Material

www.sciencemag.org/cgi/content/full/314/5803/1308/DC1
Materials and Methods
Figs. S1 to S10
References

31 May 2006; accepted 6 October 2006
10.1126/science.1130651

Predictive Codes for Forthcoming Perception in the Frontal Cortex

Christopher Summerfield,[1,2*] Tobias Egner,[3,4] Matthew Greene,[1] Etienne Koechlin,[2] Jennifer Mangels,[1] Joy Hirsch[3,5]

Incoming sensory information is often ambiguous, and the brain has to make decisions during perception. "Predictive coding" proposes that the brain resolves perceptual ambiguity by anticipating the forthcoming sensory environment, generating a template against which to match observed sensory evidence. We observed a neural representation of predicted perception in the medial frontal cortex, while human subjects decided whether visual objects were faces or not. Moreover, perceptual decisions about faces were associated with an increase in top-down connectivity from the frontal cortex to face-sensitive visual areas, consistent with the matching of predicted and observed evidence for the presence of faces.

One function of the visual system is to decide what is present in the local environment, resolving potentially ambiguous sensory information into a coherent percept. Models of perceptual decision-making propose that specialized detectors accumulate evidence in favor of a preferred feature or representation, and the output of these detectors is compared in a winner-takes-all fashion at a downstream processing stage (*1*). Accordingly, when subjects are asked to decide whether they perceive stimulus A or stimulus B, cell assemblies in the frontal and parietal cortices track the difference in output of visual neurons collecting evidence in favor of A and B (*2*, *3*).

Prior information may help the brain decide among competing percepts (*4*). According to one view, the brain generates "predictive codes" that dynamically anticipate the forthcoming sensory environment, weighting perceptual alternatives on the basis of this prediction (*5*, *6*). Predictive accounts of decision-making have long been embedded in theories of signal detection, which suggest that subjects compare observed sensory evidence against an internal "template," with a response elicited if the match between the evidence and the template reaches a given criterion (*7*). Moreover, predictive coding offers a parsimonious account for several well-known behavioral phenomena (*8*–*10*) and recent neurophysiological findings (*11*, *12*). The theory requires that decision-making neurons have access to the set of predicted information (here, we call this "perceptual set") against which to match the sensory data. However, little is known about how—or where—perceptual set might be represented in the decision-making architecture of the brain.

To address this question, we capitalized upon recent work in which functional magnetic resonance imaging (fMRI) was used to identify brain regions responsible for collecting evidence about the presence of faces on

[1]Department of Psychology, Columbia University, 1190 Amsterdam Avenue, New York, NY 10027, USA. [2]INSERM U742, Département d'Études Cognitives, Ecole Normale Superieure, 29, Rue d'Ulm, Paris, 75005, France. [3]Functional MRI Research Center, Neurological Institute, Columbia University, 710 West 168 Street, New York, NY 10032, USA. [4]Cognitive Neurology and Alzheimer's Disease Center, Feinberg School of Medicine, Northwestern University, 320 East Superior, Searle 11, Chicago, IL 60611, USA. [5]Center for Neurobiology and Behavior, Neurological Institute, Columbia University, 710 West 168 Street, New York, NY 10032, USA.

*To whom correspondence should be addressed. E-mail: summerfd@paradox.columbia.edu

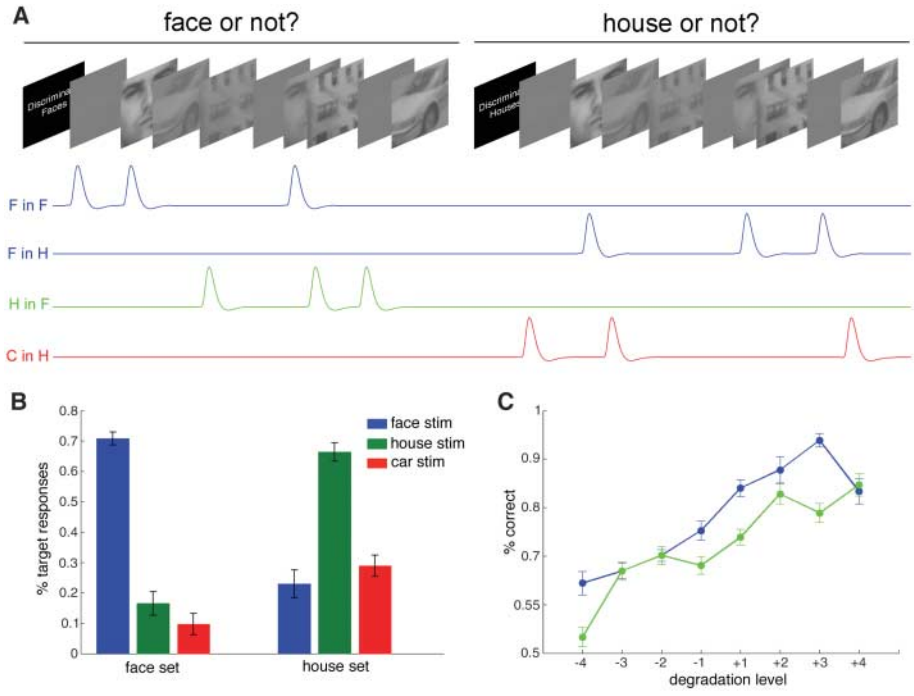

Fig. 1. Discrimination task and behavioral data. (**A**) Subjects viewed a sequence of reduced-contrast images of faces, houses, and cars. Four example regressors are shown: for example, F in F (face stimulus in face set block) or C in H (car stimulus in house set block). (**B**) Hit rate was comparable (P = 0.28) on face set blocks (left; 70.8 ± 13.4) and house set blocks (right; 66.3 ± 11.9). Moreover, on neither face set blocks (P = 0.26) nor house set blocks (P = 0.92) did hit rate deviate from pre-established thresholds for discrimination (66%). More false alarms were made on house blocks (25.9 ± 13) than face blocks (13.1 ± 10.5) [$t_{(14)}$ = 4.52, P < 0.001]. (**C**) Overall percent correct responses varied as expected with degradation level (relative to threshold) for face set blocks (blue lines) and house set blocks (green lines). Each degradation level reflects ~2% loss of contrast information. Bars are standard errors.

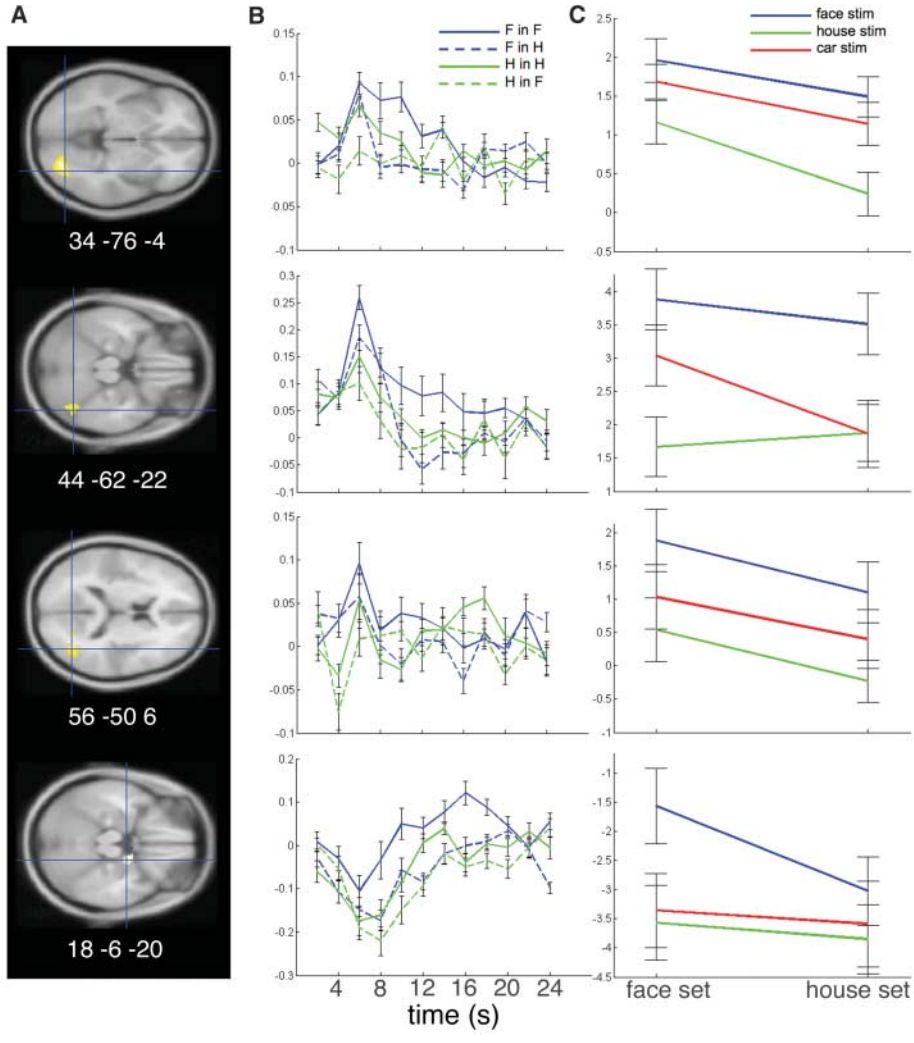

Fig. 2. IOG, FFA, TPJ, and amygdala respond to face stimuli. (**A**) (Top to bottom) Statistic parametric maps showing clusters in the IOG, FFA, TPJ, and amygdala responding to face stimuli > house stimuli at the second (group) level, rendered on a standard brain at a statistical threshold of P < 0.005 (IOG, FFA, and TPJ) or P < 0.01 (amygdala). Blue crosshairs mark the peak voxel in each cluster. (**B**) Evoked hemodynamic responses from the peak voxel in each cluster to faces (blue lines) and house (green lines), in face set (continuous lines) and house set (dashed lines) conditions. (**C**) Post hoc analyses of variance (ANOVAs) confirmed that a main effect of stimulus was observed in the IOG [$F_{(2,14)}$ = 10.8, P < 0.001], the FFA [$F_{(2,14)}$ = 8.4, P < 0.003], and the TP] [$F_{(2,14)}$ = 19.0, P < 0.0001]. In the amygdala, we observed an interaction between set and stimulus (F = 3.7, P < 0.04). Additional t tests performed on the evoked hemodynamic responses revealed an interaction between set and stimulus in the FFA, at ~12 s (F = 6.0, P < 0.03)

the inferior occipital gyrus (IOG) and the fusiform gyrus, in a region known as the fusiform face area (FFA) (*13*). The FFA exhibits neural responding that varies with subjects' beliefs about whether the stimulus is a face or not (*14*, *15*), suggesting that it is a target for "set-related" modulation during face perception. Moreover, face perception excites an "extended" network of brain regions beyond the visual cortices (*16*, *17*), including sites on the temporo-parietal junction (TPJ), amygdala, medial frontal cortices (MFCs) (*18*), and adjacent orbitofrontal cortex (*19*). This provides a number of candidate regions in which a representation of a face "set" might be observed.

To dissociate between brain regions responsible for detecting the physical presence of the stimuli and those supporting perceptual set, we used a simple task that required subjects to discriminate between randomly intermixed images of faces, houses, and cars (*20*). Although there were three object categories, subjects used just two buttons to adjudicate between them: on "face set" blocks, they judged whether each object was a face or not, and on "house set" blocks, they judged whether each object was a house or not (Fig. 1A). We also made the task perceptually challenging, by degrading stimuli to match individual thresholds for perception (66.6% correct). These manipulations encouraged subjects to generate a perceptual "set" (corresponding to the target stimulus) on each block. Because face set and house set blocks were carefully matched within subjects both for the physical characteristics of the stimuli and for discrimination performance (Fig. 1, B and C), the comparison between fMRI activity on face set blocks > house set blocks allowed us to isolate brain activity associated with maintaining a "face set" active—irrespective of whether the physical stimulus was a face, house, or car.

We first explored the effect of stimulus during the discrimination task, by comparing all face stimuli > nonface stimuli, irrespective of perceptual set. Despite the heavy perceptual degradation imposed, selectivity for the physical stimulus was preserved in face-responsive regions such as the IOG, FFA, TPJ, and amygdala (Fig. 2). However, turning to our main comparison of interest (face sets > house sets), a rather different pattern emerged: Face sets elicited greater activation in dorsal (dMFC) and ventral (vMFC) foci within the MFC, irrespective of the physical stimulus presented (Fig. 3). These MFC regions have been previously implicated in face processing in fMRI studies (*17*, *21*), and with single-unit recordings in the macaque (*18*, *19*), and overlapped with regions activated by fully visible faces in a separate experiment (fig. S1).

The images that appeared on face set and house set blocks for each subject were matched for their physical properties, and occurred with equal probability, such that observed differences in fMRI activity for face sets > house sets cannot be accounted for by the frequency, salience, or visibility of faces. Face-responsive regions of the MFC are thus involved in maintaining a predictive face "set"—information that is relevant for making perceptual decisions about faces. This result squares well with previous findings: first, the responses of face-selective neurons in the MFC are poorly synchronized with the presentation of a face (*18*), suggesting that they are not passively elicited by face presentation; second, the MFC is particularly responsive to familiar faces, for which a face "template" is presumably more readily available (*21*); and third, "top-down" generation of face-related contextual information during recall of specific face exemplars excites the vMFC (*22*). Finally, these two MFC regions are often activated when subjects make a range of perceptual, affective, or social decisions about faces (*23*, *24*).

To rule out alternative explanations of the "perceptual set" effect in MFC, we conducted a number of supplementary analyses. Because the dMFC is involved in monitoring for and detecting errors (*25*), our results could simply reflect the proportions of errors made on face set versus house set blocks. However, behavioral data (Fig. 1, B and C) indicated that hit rate did not differ between face set and house

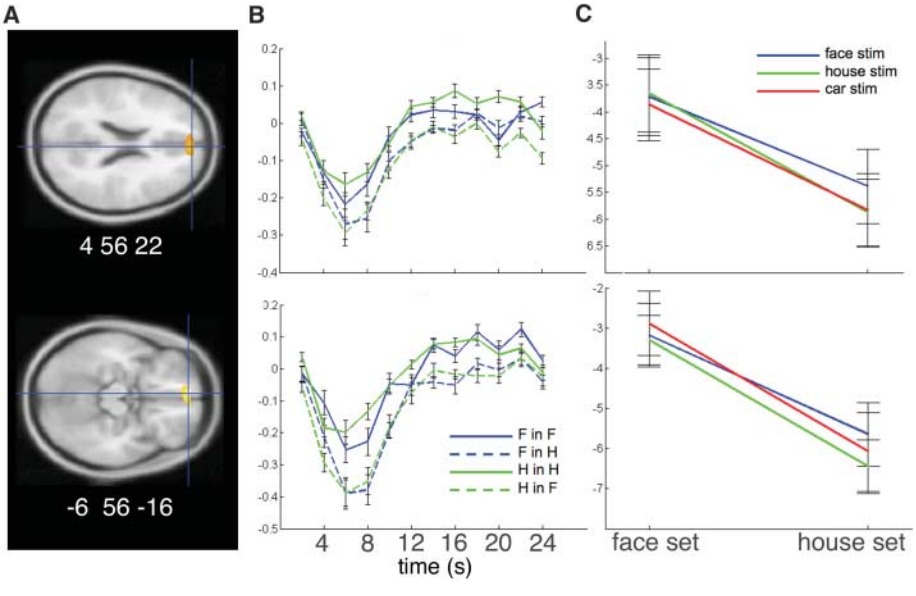

Fig. 3. dMFC and vMFC respond to face set. (**A**) Statistic parametric maps showing dMFC (top) and vMFC (bottom) voxels responding to face set blocks > house set blocks, rendered at a statistical threshold of $P < 0.01$. (**B**) Evoked hemodynamic responses, as in Fig. 2. Continuous lines are face set trials; dashed lines are house set trials. (**C**) Post hoc ANOVAs at the peak voxel in each cluster revealed a significant main effect of set [dMFC: 4, 56, 22; $F_{(2,14)} = 22.1$, $P < 0.0004$; vMFC: −6, 56, −16; $F_{(2,14)} = 20.4$, $P < 0.0005$]. No effect of stimulus was observed at either dorsal ($P = 0.70$) or ventral ($P = 0.75$) sites.

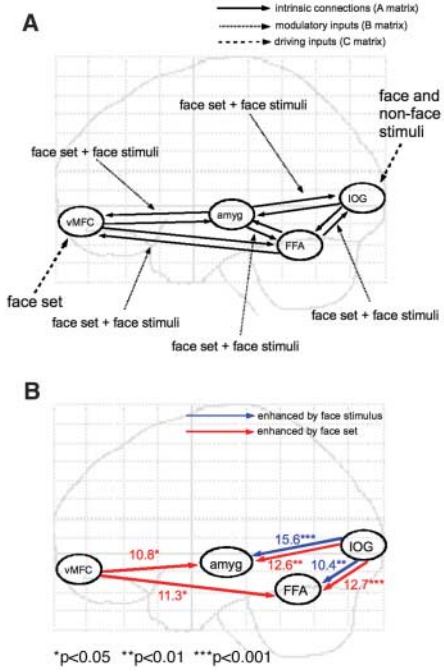

Fig. 4. Connectivity analyses. (**A**) A simple dynamic causal model with hierarchically ordered bidirectional connections between vMFC, amygdala, FFA, and IOG. We modeled face and nonface stimuli as inputs to IOG, and face sets as inputs to vMFC. (**B**) Statistically significant enhancements in connectivity due to face stimulus (blue lines) and face set (red lines) within this network. Coefficients associated with each line refer to percentage increase in connectivity relative to baseline.

set blocks, and correlation analyses showed that the number of errors made bore no relation to the neural signal in the dMFC ($P > 0.67$) or vMFC ($P > 0.45$). A second alternative account of our data relates to the role of frontal cortex in the detection of target stimuli (*25*). However, no interactions between perceptual set and response (target or nontarget) were observed in either dMFC or vMFC (fig. S2). Finally, if the MFC were simply responding to task difficulty, then a difference in fMRI signal should be observed between less degraded (easier) and more degraded (harder) trials in this region. However, neither dMFC nor vMFC activity covaried either positively or negatively with stimulus contrast (fig. S3).

Consistent with previous work (*14*, *15*), we also observed set-related effects in the posterior brain, with an advantage for face sets over house sets in the amygdala and FFA (Fig. 2). We reasoned that "top-down" signals from the MFC could sensitize visual regions responsible for collecting evidence about the presence of faces via long-range effective connectivity. To test this hypothesis, we created a simple dynamic causal model (Fig. 4A) of the interactions among visual and MFC regions, basing our model on known interconnectivity from studies of macaque neuroanatomy (*26*). Treating the brain as an input-state-output system, dynamic causal modeling estimates how (output) hemodynamic activity in a given brain region depends not only on the (input) variables manipulated by the experimenter (such as face stimulus or face set), but also on its interconnectivity with other brain regions whose activity correlates with the task. These inter-regional dependencies can then be parameterized as effective connectivity, allowing confirmatory hypothesis-testing about how brain regions interact during task performance (*27*).

Face stimulation enabled the flow of information within the posterior and limbic lobes, augmenting feedforward connections linking IOG to the FFA and amygdala. However, feedback connectivity from ventral MFC to the FFA and amygdala was significantly enhanced (by about 11% relative to baseline) on face set trials. By contrast, face set trials had no influence on bottom-up projections from the FFA ($P > 0.17$) or amygdala ($P > 0.19$) to the frontal cortex (Fig. 4B). One appealing interpretation of these data is that top-down signals originating in the vMFC may drive the increased FFA and amygdala response on face set trials—supporting recent reports that vMFC activity correlates with subjective awareness during object recognition (*28*) and that connectivity between the FFA and the frontal pole is increased when subjects generate mental images of faces (*29*).

These findings suggest that subjects do indeed deploy predictive information in the service of face perception. If subjects had been solving the three-way discrimination by accumulating evidence in favor of each of the possibilities in an unbiased way, then the comparison between brain activity for face sets and house sets would most likely have failed to yield any differences in brain activity. Moreover, a category-specific perceptual "set" can be visualized in the frontal cortex on a scale gross enough to be detected with fMRI. In supplementary analyses, we identified other frontal regions that were more active on "house set" than "face set" blocks, suggesting that this result may generalize to other categories (fig. S4).

During perceptual inference, discrete neural assemblies in the frontal cortex may come to transiently code for one or more predicted representations and send top-down signals to guide the activation in sensory regions responsible for collecting evidence about the corresponding stimuli. This long-range connectivity may underlie the matching of predictive codes for faces—maintained in the MFC—with incoming sensory data gathered in the face-sensitive zones of the extrastriate cortex, in the service of deciding whether a stimulus is a face or not.

References and Notes

1. P. L. Smith, R. Ratcliff, *Trends Neurosci.* **27**, 161 (2004).
2. J. N. Kim, M. N. Shadlen, *Nat. Neurosci.* **2**, 176 (1999).
3. H. R. Heekeren, S. Marrett, P. A. Bandettini, L. G. Ungerleider, *Nature* **431**, 859 (2004).
4. A. Wald, J. Wolfowitz, *Proc. Natl. Acad. Sci. U.S.A.* **35**, 99 (1949).
5. K. Friston, *Neural Netw.* **16**, 1325 (2003).
6. D. Mumford, *Biol. Cybern.* **66**, 241 (1992).
7. J. Swets, in *Signal Detection and Recognition*, J. Swets, D. Green, Eds. (Wiley, New York, 1964), pp. 164–171.
8. R. N. Henson, M. D. Rugg, *Neuropsychologia* **41**, 263 (2003).
9. R. H. Carpenter, M. L. Williams, *Nature* **377**, 59 (1995).
10. S. Palmer, *Mem. Cognit.* **3**, 519 (1975).
11. J. Sharma, V. Dragoi, J. B. Tenenbaum, E. K. Miller, M. Sur, *Science* **300**, 1758 (2003).
12. M. L. Platt, P. W. Glimcher, *Nature* **400**, 233 (1999).
13. N. Kanwisher, J. McDermott, M. M. Chun, *J. Neurosci.* **17**, 4302 (1997).
14. C. Summerfield, T. Egner, J. Mangels, J. Hirsch, *Cereb. Cortex* **16**, 500 (2006).
15. R. J. Dolan *et al.*, *Nature* **389**, 596 (1997).
16. J. V. Haxby, E. A. Hoffman, M. I. Gobbini, *Trends Cognit. Sci.* **4**, 223 (2000).
17. A. Ishai, C. F. Schmidt, P. Boesiger, *Brain Res. Bull.* **67**, 87 (2005).
18. S. P. Ó Scalaidhe, F. A. Wilson, P. S. Goldman-Rakic, *Science* **278**, 1135 (1997).
19. S. J. Thorpe, E. T. Rolls, S. Maddison, *Exp. Brain Res.* **49**, 93 (1983).
20. Materials and methods are available as supporting material on *Science* Online.
21. A. Todorov, M. I. Gobbini, K. K. Evans, J. V. Haxby, *Neuropsychologia* (2006).
22. S. M. Polyn, V. S. Natu, J. D. Cohen, K. A. Norman, *Science* **310**, 1963 (2005).
23. T. Singer, S. J. Kiebel, J. S. Winston, R. J. Dolan, C. D. Frith, *Neuron* **41**, 653 (2004).
24. J. P. Mitchell, C. N. Macrae, M. R. Banaji, *Neuron* **50**, 655 (2006).
25. K. R. Ridderinkhof, M. Ullsperger, E. A. Crone, S. Nieuwenhuis, *Science* **306**, 443 (2004).
26. H. Barbas, *Adv. Neurol.* **84**, 87 (2000).
27. K. J. Friston, L. Harrison, W. Penny, *Neuroimage* **19**, 1273 (2003).
28. M. Bar *et al.*, *Proc. Natl. Acad. Sci. U.S.A.* **103**, 449 (2006).
29. A. Mechelli, C. J. Price, K. J. Friston, A. Ishai, *Cereb. Cortex* **14**, 1256 (2004).

30. Financial support was from the William J. Keck Foundation and the NIH (grant R21066129).

Supporting Online Material

www.sciencemag.org/cgi/content/full/314/5803/1311/DC1
Methods
Figs. S1 to S4
References

3 July 2006; accepted 20 October 2006
10.1126/science.1132028